Thermodynamic and Kinetic Studies of DNA Triplex Formation of an Oligohomopyrimidine and a Matched Duplex by Filter Binding Assay†

Heisaburo Shindo,*,‡ Hidetaka Torigoe,§ and Akinori Sarai§

Tokyo College of Pharmacy, Hachioji, Tokyo 192-03, Japan, and Laboratory of Gene Bank, Tsukuba Life Science Center, Institute of Physical and Chemical Research (Riken), Tsukuba 305, Japan

Received March 25, 1993; Revised Manuscript Received May 12, 1993

ABSTRACT: The filter binding method was found to be a powerful method for studying the formation of triplexes composed of a single-stranded homopyrimidine and a duplex with a matched purine–pyrimidine tract. With this technique, we were able to determine thermodynamic and kinetic parameters for triplex formation between a homopyrimidine 19-mer (5′-TCCTCTTCTTTTCTTTCTT-3′) and a duplex with sequence 5′-GCAGGAGAAGAAAAGAAAGAACG-3′ for the purine strand. The experiments were performed over a wide pH range (3.8–7.4) and a temperature range of 0–35 °C. pH and temperature dependencies of the thermodynamic parameters were best explained in terms of a three-state model for triplex formation at low temperatures relative to the melting point. The main results were as follows: (1) pH dependence of the dissociation constants of the triplex is a result of the rapid acid–base equilibrium of pyrimidine single strands; (2) the association rate for triplex formation decreases with increasing pH in accordance with the dissociation constants; (3) the dissociation constant is virtually temperature-independent at low pH, while it becomes strongly temperature-dependent with increasing pH (these results can be explained in terms of a negative, non-zero ΔC_p for triplex formation at low pH); (4) the association rate decreases with increasing temperature, and the resulting negative activation energy indicates that the triplex formation process involves a quasi-stable intermediate; (5) the triplex formation is a second-order reaction at low pH, whereas it can be interpreted as a third-order reaction at neutral pH, suggesting that different triplex formation pathways are observed depending on the pH.

There has been increasing interest in the study of triplex formation, which is regarded as one of the most versatile methods for recognition of double-helical DNA sequences [see reviews by Moser and Dervan (1987) and Wells et al. (1988)]. In a triplex, the pyrimidine nucleotide binds to the purine tract in the major groove of the duplex by forming specific Hoogsteen-type hydrogen bonds with the purine bases (Arnott & Selsing, 1974; Rajagopal & Feigon, 1989; de los Santos et al., 1989; Macaya et al., 1992; Radhakrishnan et al., 1992). The high stability of the triplexes and their base sequence specificity makes it possible to create a powerful method for recognizing a single site within a large segment of double-stranded DNA. For example, triplexes have been used to mediate site-specific cleavage of human chromosomal DNA (Strobel et al., 1991) as well as to inhibit particular transcription *in vitro* (Mahr, 1992; Cooney et al., 1988; Kohwi & Kohwi-Shigematu, 1991; Postel et al., 1991; Grigoriev et al., 1992; McShan et al., 1992).

Because of the potential applications of, and the fundamental interest in, the triplex formation mechanism, numerous studies have been carried out recently to elucidate the factors contributing to the stabilities and specificities of a variety of triplexes. The triplex formations were monitored by many different techniques such as UV–melting (Durand et al., 1992; Rougee et al., 1992; Xodo et al., 1990, 1991; Mergny et al., 1991), differential scanning calorimetry (DSC) (Plum et al., 1990), gel electrophoresis (Yoon et al., 1992; Hampel et al., 1991; Roberts & Crothers, 1991), affinity cleavage (Singleton & Dervan, 1992a,b; Collier et al., 1991; Kiessling et al., 1992; Beal & Dervan, 1991; Perrouault et al., 1990; Griffin & Dervan, 1989), footprinting and enzymic cleavage (Krawczyk et al., 1992; Nielsen et al., 1991; Mahr et al., 1990), column chromatography (Ito et al., 1992), and so on. However, we are still far from fully understanding the effects of such simple factors as pH, temperature, and base composition. Therefore, more complete characterizations of both the thermodynamics and kinetics of triplex formation need to be made. To date, only a few kinetic studies have been reported (Maher et al., 1990; Rougee et al., 1992).

UV–melting and DSC are considered to be the most suitable techniques for thermodynamic studies. However, they operate best near the triplex melting temperature, T_m. As such, the thermodynamic parameters obtained will not always reflect the true features of triplexes at temperatures far below or far above T_m. Since the stability of triplexes is most correctly defined by the Gibbs free energy, $\Delta G°$, a technique for directly measuring $\Delta G°$ or the dissociation constant, K_d, is desired. The last four methods mentioned above, such as gel electrophoresis, can measure $\Delta G°$ and K_d, but they are restricted in their ability to monitor kinetic problems because of their low time resolution (Maher et al., 1990).

In this study, we demonstrate that the filter binding method, which has been widely used for studying protein–DNA interactions, is a powerful method for studying the thermodynamics and kinetics of triplex formation at temperatures far below T_m and over a wide pH range. Thermodynamic and kinetic data were relatively readily obtained for a triplex system using this method. Temperature and pH dependencies of the system were analyzed and discussed in terms of a three-state model.

† This work was supported in part by a Grant-in-Aid for Scientific Research from the Ministry of Education, Science and Culture of Japan (04254105).

* Author to whom correspondence should be addressed.
‡ Tokyo College of Pharmacy.
§ Institute of Physical and Chemical Research.

0006-2960/93/0432-8963$04.00/0

MATERIALS AND METHODS

Oligodeoxyribonucleotides were synthesized with a 381A DNA synthesizer (Applied Biosystems) and then purified by HPLC according to the Applied Biosystems protocol. Equimolar amounts of two complementary nucleotides (23 nt), determined on the basis of an ultraviolet (UV) titration curve, were mixed into a solution containing buffer (50 mM NaCl and 10 mM Tris-HCl, pH 7.5). The sample was annealed by heating to 90 °C, followed by gradual cooling to room temperature. The concentrations of the double-stranded DNA 23-mer were determined by the UV absorbance to DNA concentration ratio of 1 OD = 50 μg/mL, with a molecular weight of 650 assigned to each base pair. Base sequences of the duplexes (pur·pyr23AT and pur·pyr23GC) and homopyrimidine strands were as follows:

pur·pyr23GC	5′-GCAGGAGAAGAGGAAAAAGAACG-3′
	3′-CGTCCTCTTCTCCTTTTTCTTGC-5′
pyr19C	5′-TCCTCTTCTCCTTTTTCTT-3′
pyr15C	5′-CTCTTCTCCTTTTTC-3′
pyr12C	5′-TCTTCTCCTTTT-3′
pyr10C	5′-CTTCTCCTTT-3′
pur·pyr23AT	5′-GCAGGAGAAGAAAAGAAAGAACG-3′
	3′-CGTCCTCTTCTTTTCTTTCTTGC-5′
pyr19T	5′-TCCTCTTCTTTTCTTTCTT-3′

The filter binding method used here was essentially the same as the one commonly used for studying protein–DNA complexes (Riggs et al., 1970) briefly described below. The single-stranded pyr19T was ^{32}P-end-labeled, and an aliquot of purified pyr19T was added to a series of Eppendorf tubes, each containing 100 μL of the binding buffer (225 mM NaCl, 20 mM acetate, 20 mM cacodylate, and 20 mM Tris-HCl at desired pH). Varying amounts of pur·pyr23AT were added to the binding buffer and incubated at a specific temperature for 1 h. The samples were then passed through nitrocellulose filters (Schleider & Schuell, BA-85, 0.45 μm) under suction. The filters were dried and assayed by a liquid scintillation counter.

To measure the association rate, a large amount of duplex 23-mer (pur·pyr23AT) was added to a solution containing ^{32}P-end-labeled single-stranded 19-mer (pyr19T) and then stirred rigorously. After the addition of the duplex 23-mer, an aliquot of the solution (100 μL) was filtered through a nitrocellulose membrane over a series of time intervals. The filters were dried and assayed by a liquid scintillation counter.

THEORETICAL CONSIDERATIONS

Triplex formation is achieved by forming Hoogsteen hydrogen bonds between the homopyrimidine and the matching purine–pyrimidine tract in a DNA duplex. Completely matched triplets are thymine and protonated cytosine with A·T and G·C Watson–Crick base pairs, respectively (de los Santos et al., 1989; Rajagopal & Feigon, 1989; Pilch et al., 1990). Because the cytosines must be protonated before the triplex can be formed, the stability of the triplex depends heavily on pH. Lyamihev et al. (1988) have developed a theory to explain the pH-dependent structural transition of intramolecular triplexes that are under supercoiled stress in plasmids. The theory includes a dramatic transition in which the intramolecular triplex forms after disruption of the Watson–Crick duplex. The application of this theory to intermolecular triplexes (Singleton & Dervan, 1992b) is somewhat complicated because the theory involves many unknown parameters. As such, we will describe an alternate, simple theory suitable for analyzing intermolecular triplex formations.

If we assume that duplex D forms triplex T with single-stranded homopyrimidine S, and that the process is reversible and involves an intermediate state SD*, then the process can be expressed by a three-state model as follows:

$$S + D \rightleftarrows SD^* \rightleftarrows T \quad (1)$$

In the case where the third strand contains cytidyl residues, the single strand with positively charged cytosines, S′, is supposed to form the triplex exclusively. Then, the reaction equilibrium may be written as follows:

$$S' + D \underset{k_2}{\overset{k_1}{\rightleftarrows}} SD^* \underset{k_4}{\overset{k_3}{\rightleftarrows}} T$$

$$S' \rightleftarrows S + nH^+ \quad K_a \quad (2)$$

where k_1 and k_2 represent the association and dissociation rate constants, respectively. The association may be referred to as the nucleation process used to describe the formation of double-stranded RNA from two complementary single strands (Craig et al., 1971; Ross & Sturtevant, 1962). Similarly, k_3 and k_4 represent the chain growth and chain opening rate constants, respectively, the former of which may also be called the zip-up rate, and the latter the chain breaking rate (Craig et al., 1971). Reaction 2 is a rapid acid–base equilibrium. The dissociation constant K_a refers to cytidyl residues in the third strand. The pK_a was reported to be about 4.5 (Xodo et al., 1991). Parameter n may be a value from 0 up to the number of cytidyl residues within the third strand and perhaps depends on the state of the intermediate. That n can equal 0 implies that the third strand is composed of thymidyl residues only or that no protonation of cytidyl residues is required for the formation of SD*.

The equilibrium constant for the dissociation of triplex T can be written as

$$K_d = [S'][D]/[T] \quad (3)$$

The total concentration of the single strand, free from the complex, is assumed to be assayed by a nitrocellulose membrane filter as follows:

$$[S]_f = [S'] + [S] = [S'](1 + K_a/[H^+]^n) \quad (4)$$

Thus, the apparent dissociation constant K_d' is given by

$$K_d' = [S]_f[D]/[T] = K_d/\alpha \quad (5)$$

where

$$\alpha = [H^+]^n/([H^+]^n + K_a) \quad (6)$$

K_d' can also be expressed in terms of the rate constants as

$$K_d' = k_2k_4/k_1k_3\alpha \quad (7)$$

Equation 5 indicates that the observed dissociation constant, K_d', equals the thermodynamic dissociation constant K_d when $[H^+]^n \gg K_a$ in acidic medium, whereas K_d' increases with increasing pH. This is an essential feature of the pH dependence of DNA triplex stability.

Association and dissociation rates can be assayed by filter binding experiments. Association rates can be measured from the decay curve of free single strands after the addition of enough double-stranded DNA to complete triplex formation. Rates of formation of the free single strands and intermediates can be expressed as differential equations with respect to time

as follows:

$$d[S]_f/dt = d[S']/dt + d[S]/dt$$
$$= -k_1[S'][D] + k_2[SD^*]$$
$$= -k_1\alpha[S]_f[D] + k_2[SD^*] \quad (8)$$

$$d[SD^*]/dt = k_1[S'][D] - (k_2 + k_3)[SD^*] + k_4[T]$$
$$= k_1\alpha[S]_f[D] - (k_2 + k_3)[SD^*] + k_4[T] \quad (9)$$

Since it is reasonable to assume that triplex T is sufficiently stable such that $k_4 \ll k_1$, k_2, and k_3, the following differential equation can be derived after taking the second derivative of eq 8, followed by substitution and rearrangement of eqs 8 and 9:

$$d^2[S]_f/dt^2 + (k_1[D]\alpha + k_2 + k_3)d[S]_f/dt + k_1k_3[D]\alpha[S]_f = 0 \quad (10)$$

Since $[D] \gg [S]_f$ in the experiment, [D] is considered to be constant. Thus, eq 10 can be solved with respect to the variable $[S]_f$ to give the following general solution:

$$[S]_f = C_1 \exp(\lambda_1 t) + C_2 \exp(\lambda_2 t) \quad (11)$$

where $\lambda_1 = -h - (h^2-k^2)^{1/2}$, $\lambda_2 = -h + (h^2-k^2)^{1/2}$, $h = {}^1/_2(k_1[D]\alpha + k_2 + k_3)$, and $k = (k_1k_3\alpha[D])^{1/2}$. Initial conditions are $[S]_f = [S]_0$ and $d[S]_f/dt = -k_1[S]_0[D]\alpha$ at $t = 0$. Here, $[S]_0$ is the initial concentration of the pyrimidine single strands. Coefficients C_1 and C_2 in eq 11 are as follows:

$$C_1 = (-\lambda_2 - k_1[D]\alpha)/(\lambda_1 - \lambda_2)[S]_0 \quad (12)$$

$$C_2 = (\lambda_1 + k_1[D]\alpha)/(\lambda_1 - \lambda_2)[S]_0 \quad (13)$$

It is worthwhile to consider a special case for later discussion. If the chain growth rate is much slower than the association rate constant, i.e., $k_1[D]\alpha \gg k_3$, then eq 11 can be simplified to the following:

$$[S]_f = (k_2/\beta)[S]_0 \exp(-k_1k_3[D]\alpha/\beta t) + (k_1[D]\alpha/\beta)[S]_0 \exp(-\beta t) \quad (14)$$

where $\beta = k_1[D]\alpha + k_2$. Since α is 1 at low pH and becomes smaller with increasing pH, the first term in eq 14 will dominate at acidic pH, while the second term becomes important in the neutral pH range. Furthermore, since the intermediate state SD* would be considerably stable in acidic pH as will be discussed later, the condition $k_1[D]\alpha \gg k_2$ would be assumed, and therefore eq 14 can be approximated as

$$[S]_f = [S]_0 \exp(-k_1[D]\alpha t) \quad (15)$$

RESULTS AND DISCUSSION

The filter binding assay has been commonly used to study the binding affinity of proteins to DNA (Riggs et al., 1970). The proteins and protein–DNA complexes are trapped on the nitrocellulose membrane filter, while DNA passes through it. We have found that single-stranded DNA is usually retained on the nitrocellulose membrane filter. The retention efficiency of the filter was around 45–65% for single-stranded homopyrimidines and less than 10% for double- and triple-stranded DNAs. The efficiency was affected by filtering speed, temperature, pH, and probably base sequences. It was somewhat surprising that only 10% or less of the single-stranded homopurines were retained, which was almost the same amount of double-stranded DNA retained. This is probably because homopurines may take on a defined structure in solution (Saengar, 1984).

Effects of the Length of the Third pry Strand on DNA Triplex Formation. Figure 1 shows a series of titration curves

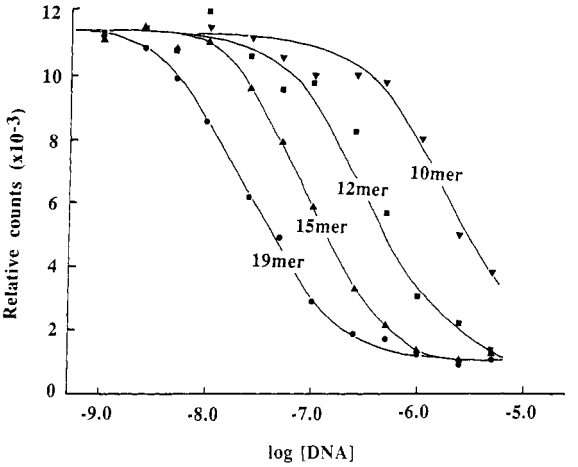

FIGURE 1: Plots of relative counts in cpm of ^{32}P-end-labeled homopyrimidines with different lengths vs. logarithm of duplex pur·pyr23GC (mol/L) assayed at 15 °C and pH 5.0 by filter binding experiments. The numbers of nucleotide bases are indicated in the figure. Apparent dissociation constants K_d' were obtained from the midpoint (i.e., DNA concentration at 6000 cpm) of each titration curve.

for ^{32}P-end-labeled pyrimidine strands with different lengths plotted as a function of double-stranded DNA 23-mer (pur·pyr23GC) concentration. Radioactivity in cpm retained on the filter was roughly adjusted to ca. 10^4 cpm in the absence of the DNA 23-mer. As shown in each curve in Figure 1, the count decreases with increasing DNA concentration and plateaus at around 10^3 cpm, indicating that all of the single-stranded homopyrimidines formed the triplexes. It is apparent that the DNA concentration at the midpoint of each titration curve, which corresponds to the half-saturation point, gives an apparent dissociation constant K_d', since the concentration of single-stranded homopyrimidines (10^{-11}–10^{-10} M) is much smaller than that of the DNA 23-mer.

The observed K_d values are in the range of 3.5×10^{-9} to 4.0×10^{-6} and vary by 2 orders of magnitude between 19-mer and 10-mer. Such an observed length dependency clearly demonstrates that the filter binding method assays the triplex formation. The stability of the triplex in free energy change per base was found to decrease from 0.69 to 0.15 kcal/base when the third pyr strand changes in length from 10 to 19 nt, suggesting that the longer pyr strand is more stabilized, but it may weaken base specificity for the triplex formation.

Effects of pH on DNA Triplex Formation. Figure 2 shows a series of titration curves for ^{32}P-end-labeled pyrimidine 19-mer (pyr19T) plotted as a function of double-stranded DNA 23-mer (pur·pyr23AT) concentration. The dissociation constants K_d' were measured from the midpoint of each titration curve and the resulting values are listed in Table I. It should be noted that the sigmoidal shape of the titration curves in Figure 2 sharpens with increasing pH as if the triplex formation becomes cooperative. This sharpening is unexpected since the triplex should be a 1:1 complex of the single-stranded and double-stranded DNA. To account for this fact, triplex formation should be regarded as a bimolecular reaction (discussed later).

The negative log of the observed K_d' values is plotted as a function of pH in Figure 3. Two points should be noted. First, the value of $-\log K_d'$ decreases with increasing pH, and second, this value seems to level off at both the lowest pH and highest pH studied. The solid line in the figure is a best fit curve obtained by eq 5, where the parameter n is constant irrespective of pH. The thermodynamic dissociation constant $K_d = 5.2 \times 10^{-9}$ M and $n = 1.1$ were used for drawing the best fit curve for the data. The value $n = 1.1$ implies that protonation of

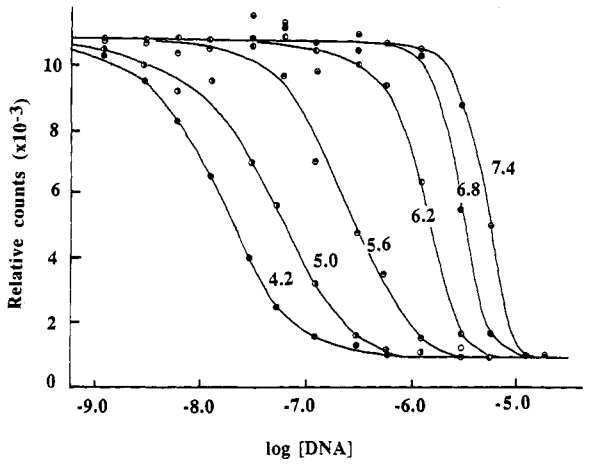

FIGURE 2: Representative plots of relative counts in cpm of ^{32}P-end-labeled pyr19T vs logarithm of duplex pur·pyr23AT (mol/L) assayed at 15 °C and at different pH values by filtering binding experiments. pH values studied are presented in the figure.

Table I: Measured Dissociation Constants K_d', Standard Thermodynamic Parameters, and Hill Coefficients for the Triple-Helix Formation of the Pyrimidine Single-Stranded 19-mer (pyr19T) with Duplex 23-mer (pur·pyr23AT)

pH	K_d' (×10^8)[a] at 15 °C	Hill coeff[b]	$\Delta G°$ [c] (kcal/mol)	K_{assoc} (×10^{-6})[d] at 25 °C
5.0	2.4 ± 0.2	1.3	−10.4	43
5.6	15.8 ± 2	1.5	−9.2	5.4
5.8	40.0 ± 4	1.7		
6.2	107 ± 10	2.3	−7.7	0.46
6.8	275 ± 20	2.7	−7.0	0.14

[a] Observed dissociation constants at 15 °C. [b] Errors may be large at pH 6.2 and 6.8. Refer to text. [c] Values at standard temperature (25 °C). [d] Association constants at 25 °C calculated from $\Delta G°$.

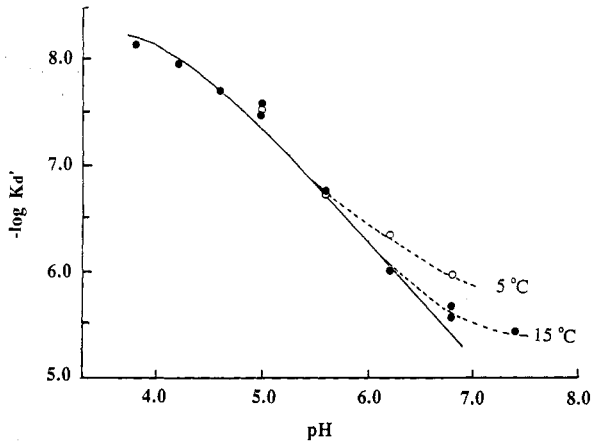

FIGURE 3: pH dependence of dissociation constant K_d' measured at two different temperatures. The solid line represents the best fit curve in the acidic pH range according to eq 5 at 15 (●) and 5 °C (○).

only one of six cytidyl residues within pyr19T is required for nucleation in the triplex formation. This result seems reasonable, assuming that the filter binding method can measure the nucleation step and that 3–4 base pairings are necessary to form the nuclei as intermediates (Craig et al., 1971). As shown in Figure 3, the theoretical curve produced a good fit with the data points in the acidic pH range. However, increasing deviation is observed in the neutral pH range where the slope becomes gentler, indicating that above pH 6 the n value is not constant and decreases with increasing pH. By extrapolating the data to pH 8 or higher, n would become 0 (i.e., K_d' is independent of pH), suggesting that another

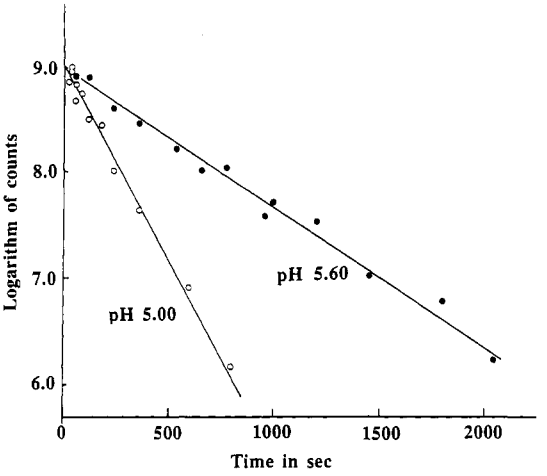

FIGURE 4: Data from association experiments for the triplex formation of ^{32}P-end-labeled pyr19T with duplex pur·pyr23AT. Radioactivity in cpm was plotted as a function of time after the addition of a large amount of the duplex at pH 5.0 and 5.6.

reaction pathway for triplex formation, different from that in the acidic pH range, occurs.

As mentioned above, the pH dependence of K_d' suggested that the filter binding method assays the nucleation step in triplex formation. In order to clarify this in more detail and to understand further the mechanism of triplex formation, it is necessary to study the kinetic parameters involved.

To measure association rates, a large amount of duplex 23-mer was added to a solution containing ^{32}P-end-labeled, single-stranded 19-mer and then stirred rigorously. An aliquot of the solution (100 μL) was filtered through a nitrocellulose membrane over a series of time intervals. The radioactivity in cpm was calculated by subtracting the equilibrium background count from the total count observed at time t. The log of this calculated value is plotted as a function of time in Figure 4. Here, 1.2×10^{-6} and 1.51×10^{-6} M of the duplex 23-mer was added for pH 5.0 and 5.6, respectively. As can be seen in Figure 2, these concentrations are large enough to complete the triplex formation in equilibrium. It seems clear from Figure 4 that the linearity of the lines implies a single exponential decay for the radioactivity retained on the membrane filter, from which the time constants 3.7×10^{-2} and 1.30×10^{-2} s^{-1} were obtained for pH 5.0 and 5.6, respectively. It appears that the rate constants are indeed pH-dependent, as expected from eq 15, and that they can be attributed to $k_1\alpha$[D].

If we assume that the rate constant k_1 does not vary at pH 5.0 or 5.6 and that pK_a = 4.5, then parameters n = 1.03 and $k_1 = 1.7 \times 10^5$ s^{-1} M^{-1} are obtained. The value n = 1.03 is in good agreement with n = 1.1 obtained from the pH-dependent K_d', as shown in Figure 3.

Temperature Dependence of Dissociation Constants. Figure 5 shows the temperature dependence of the titration curves at pH 5.0 and 6.8. In Figure 6, the negative log of the dissociation constant K_d' at various pH values is plotted against the reciprocal of the absolute temperature. It appears from Figures 5 and 6 that K_d' is virtually temperature-independent at pH 5.0, whereas it becomes temperature-dependent with increasing pH.

Using basic thermodynamic equations, $\Delta G° = -RT \ln K_{assoc} = RT \ln K_d'$ and $\Delta G° = \Delta H° - T\Delta S°$, the enthalpy change $\Delta H°$ can be calculated by assuming that it is temperature-independent. The enthalpy change calculated from van't Hoff plots in Figure 6 varies from 0 to −15.8 kcal/mol as the pH increases from 5.0 to 6.8. The relatively small absolute values of enthalpy changes obtained for low pH do not seem

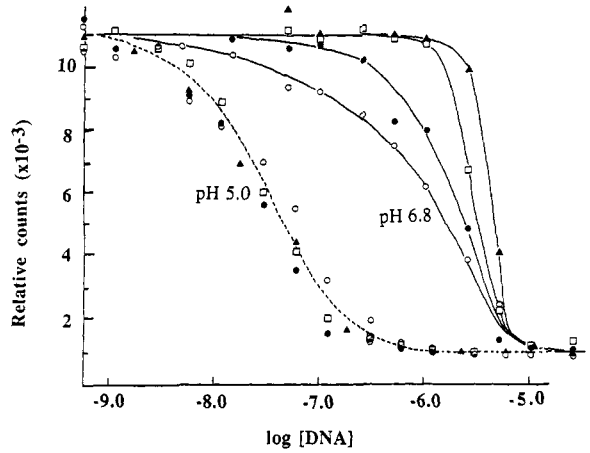

FIGURE 5: Temperature effects on the titration curves of the triplex formations at pH 5.0 and 6.8: (○) 5 °C, (●) 15 °C, (▲) 25 °C, and (□) 35 °C for the data at pH 5.0; (○) 5 °C, (●) 10 °C, (□) 15 °C, and (▲) 25 °C for the data at pH 6.8.

reasonable, since direct measurements of enthalpy changes for thermal disruption of triplexes were reported to yield about 6 kcal per base triplet at pH 5.0 (Xodo et al., 1991) and about 2 kcal per base triplet at pH 6.8 (Plum et al., 1990).

The inconsistency between our data and those obtained from DSC experiments is fundamental, suggesting that enthalpy and entropy changes may not be temperature-independent for triplex formation under the conditions studied here. It should be noted that such a temperature-dependent enthalpy change is generally found in the helix–coil transition equilibrium of proteins [see, for example, Privalov and Khechinashvili (1974)]. In fact, according to our preliminary calorimetric study using differential titration calorimetry (DTC), the enthalpy change measured in the triplex formation with a homopyrimidine 15-mer was temperature-dependent at pH 4.9, while it was not temperature-dependent at pH 6.3. The observed temperature dependence of the enthalpy change at pH 4.9 yielded an average ΔC_p value of –0.6 cal/K/mol, whereas the ΔC_p was negligible within experimental error at pH 6.3. Using the thermodynamic relation, $\Delta G° = -RT \ln K_{assoc} = \Delta H° - T\Delta S°$, the differential equation for the association constant K_{assoc} ($=1/K_d'$) for triplex formation becomes as follows, if ΔC_p is non-zero.

$$d(\ln K_{assoc})/dT = -\Delta H°/RT^2 + \Delta C_p/RT \qquad (16)$$

Since both $\Delta H°$ and ΔC_p are negative, it is possible to have a case where two of the terms in eq 16 cancel each other out, implying that the association constant is temperature-independent. Since this is the case for the triplex formation studied at pH 5.0, the standard enthalpy $\Delta H°$ is calculated to be –87 kcal/mol by taking the term on the left-hand side in eq 16 as zero and substituting a ΔC_p value of –0.6 kcal/K/mol. This calculated value is within the range between enthalpy changes of about –40 and –110 kcal/mol for triplex formation with the pyr strand 19-mer estimated from the calorimetric data (Xodo et al., 1991; Plum et al., 1990).

The non-zero, negative ΔC_p strongly suggests that hydrophobic interactions are involved in triplex formation and/or that the single-stranded pyrimidine has a defined structure at low pH and low temperature. The latter rationale is more likely the case. There are several lines of evidence indicating that both the homopurine and homopyrimidine single strands are not completely in random conformation, but have more or less defined structures at low pH and low temperature (Robinson et al., 1992; Saenger, 1984). Typical examples are the existence of a defined double-stranded polycytidine

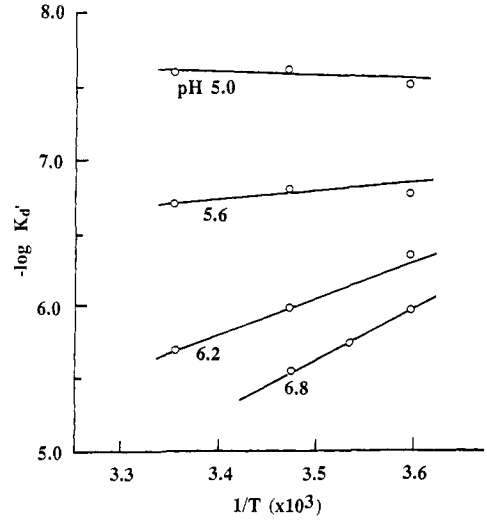

FIGURE 6: van't Hoff plots of dissociation constant K_d' at various pH values, as shown in the figure.

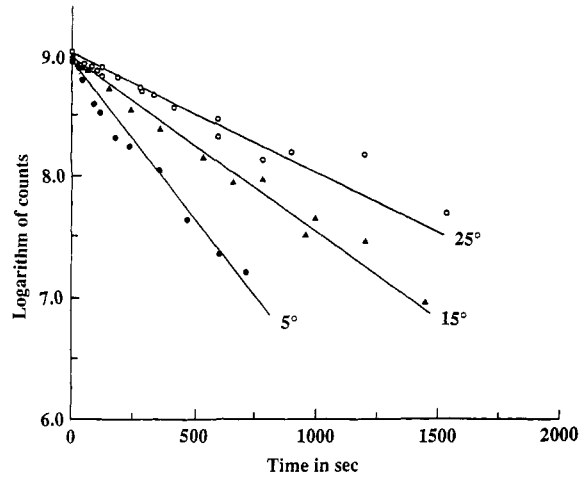

FIGURE 7: Temperature effects on the association rates for triplex formation at pH 5.8.

structure (Borah & Wood, 1976) and a single-helical polyadenosine structure (Holcomb & Tinoco, 1965) at low pH. This lack of randomness in the third strand should reduce the absolute value of the negative enthalpy change that accompanied triplex formation.

It is reasonable to assume that, as the temperature increases, the conformational energy of the third strand will be gradually released, increasing the conformational randomness. Thus, triplexes studied at higher pH values will result in more negative enthalpy and entropy changes for the triplex formation.

Temperature Dependence of Association Rates. The temperature dependence of the association rate was also examined. Figure 7 shows a single exponential decay of the radioactivity and demonstrates that the association rate increases with decreasing temperature. The resulting rate constant $k_1\alpha$ was 2.1×10^3, 1.2×10^3, and 0.8×10^3 s^{-1} M^{-1} at 5, 15, and 25 °C, respectively. log $k_1\alpha$ vs $1/T$ is plotted in Figure 8. The negative activation energy obtained from this plot was –7.6 kcal/mol. Negative activation energy was previously reported in the T-jump studies on RNA duplex formation from two complementary single-stranded RNAs (Blake et al., 1968; Porschke & Eigen, 1971; Craig et al., 1971) and in the UV-melting study of triplex formations (Rougee et al., 1992). The explanation for this negative activation energy in the formation of the RNA duplex was based on two facts: the rate-determining step is chain growth

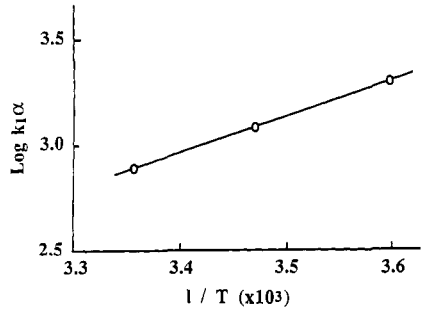

FIGURE 8: Plots of the logarithm of the association rate constant $k_1\alpha$ vs the reciprocal of the absolute temperature at pH 5.8.

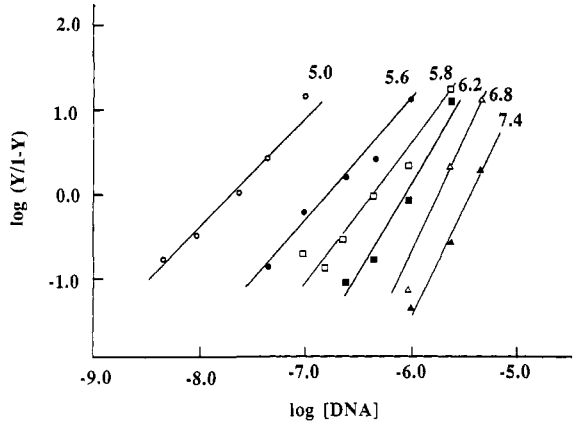

FIGURE 9: Hill plots calculated from the titration curves at 15 °C and various pH as shown in Figure 2. Variable Y represents the fraction of the triplex relative to the total fraction of pyr19T, and the numbers shown in the figure are pH values. Hill coefficients obtained from the slopes are presented in Table I.

after the formation of the intermediate complex, and pre-equilibrium exists between the dissociated state of the third strand and the intermediate complex state. The concentration of the intermediate naturally decreases with an increase in temperature, and if the rate of the decrease outweighs any advantage in the collision rate between the single strand and the duplex, which may be given by a rise in temperature, a net negative temperature coefficient is understandable. It is obvious that more kinetic data must be obtained before the intermediate states can be analyzed quantitatively.

Reaction Mechanism of Triplex Formation in the Neutral pH Range. As mentioned before, the titration curves shown in Figure 2 reveal a cooperative phenomenon in the triplex formation at high pH. The degree of cooperativity may be expressed by the so-called Hill parameter. Figure 9 shows Hill plots where Y represents a fraction of the triplex. The Hill coefficient was obtained by measuring the slopes in Figure 9, which are listed in Table I. It is evident from the table that the Hill coefficient is nearest 1 at pH 5.0, while it is about 2 in the neutral pH range. That the Hill coefficient can be 2 implies that the formation of triplex is proportional to the square of the duplex concentration. This can be seen in Figure 10A, which shows association rates at different DNA duplex concentrations added at pH 5.8. As shown in Figure 10B, the rate constant plotted against log [DNA] yielded a slope of 1.85, the value of which nearly agrees with the Hill coefficient of 1.7 at pH 5.8 from Figure 9.

Hill coefficients larger than 1 have been explained in terms of the cooperative phenomenon in enzymatic activity that is found, for example, in the binding of oxygen to hemoglobin. Since cooperative phenomena are often seen in enzymes having multiple substrate binding sites, this model cannot be applied to the DNA triplex. Another example showing cooperativity

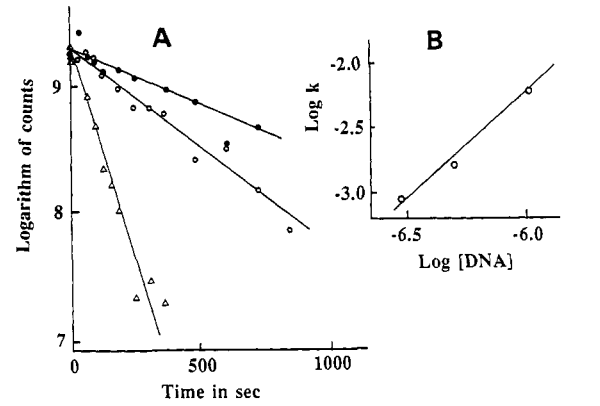

FIGURE 10: Data from association experiments for triplex formation at 15 °C and pH 5.8 (A) and log of the decay constant k vs duplex concentration added (B). Symbols for the concentrations of the duplex pur·pyr23AT: (●) 1.45×10^{-6} M; (○) 2.3×10^{-6} M; (△) 4.5×10^{-6} M.

involves the so-called memoric enzymes. It is well-known that the memoric enzyme is categorized as a protein having two distinct forms with a slow interconversion rate: enzymatically active and inactive forms. It is obvious that this model cannot be applied to triplex formation.

There is a third model for explaining large Hill coefficients. Third-order reactions are, in general, found to be comparatively very rare. However, dynamic or chemical restrictions may necessitate the occurrence of this third-order reaction. All of the third-order reactions hitherto investigated belong to one of the following categories (Moelwyn-Hughes, 1961): (1) gas-phase reactions where oppositely charged ions and similar atoms combine and (2) specific reaction types such as $2NO + O_2 \rightleftarrows 2NO_2$. The latter type of reaction has aroused great interest because, in addition to its third-order characteristics, its velocity constant was found to decrease with an increase in temperature. This also occurs in triplex formation. The negative temperature coefficient of the velocity can be explained as described above. The essential features of this type of reaction include a quasi-stable intermediate, NO_3, the rapid establishment of the equilibrium $NO + O_2 \rightleftarrows NO_3$, and additional collisions between NO_3 and NO to form nitric dioxides.

Using the above reaction as an analogy, the following scheme is proposed to explain our kinetic data for triplex formation in the neutral pH range:

$$S + D \rightleftarrows SD^* \rightarrow T \quad (17)$$

$$SD^* + D \rightarrow T + D \quad (18)$$

Here, S represents the single-stranded pyrimidine, free from the complex, and SD* represents quasi-stable intermediates. At low pH, the chain growth rate (SD* → T) would be high because of the relatively high concentration of positively charged S. At high pH, however, this rate would be highly restricted because all of the cytidyl residues on the relatively long chain segment must be protonated. As demonstrated above, the rate of triplex formation was nearly proportional to approximately the square of the duplex concentration at pH 5.8. This result, therefore, suggests that reaction 18 would predominate over the chain growth pathway in reaction 17. In reaction path 18, duplex D may serve as a self-catalyst as well as the reactant for triplex formation. Although details of the catalytic mechanism are not known, the following model may be a possibility: Initially, a duplex binds a part of a segment of the pyrimidine strand to form an intermediate complex. Then, triplex formation might be accelerated by

the collision or binding of another duplex to the unbound portion of the pyrimidine strand.

CONCLUDING REMARKS

At the end of the 1960s, the reaction mechanisms of double-helix formation were studied extensively both theoretically and experimentally (Craig et al., 1971; Porschke & Eigen, 1971; Blake et al., 1968; Blake & Fresco, 1966). Although researchers often found it difficult to define the intermediate complex for interpreting the kinetic data obtained by a variety of methods, negative activation energy demonstrated the existence of intermediate states (nucleation) in the duplex formation processes. The same was true in the triplex formation studied here and elsewhere (Rougee et al., 1992). The essential difference between duplex and triplex formations is that the triplex formation is strongly pH-dependent because the cytidyl residues in the third strands need to be protonated.

pH dependencies of the dissociation constant and the association rate for triplex formation were strong in the acidic pH range (pH 4–6), but became absent at pH 8 or higher. These results led us to conclude that in the acidic pH range the rate-determining steps (nucleation and/or chain growth) required protonation of only some of the cytidyl residues within the third strand, while in neutral and basic pH ranges the triplex formation became nearly independent of pH.

The dissociation constant was virtually temperature-independent at pH 5.0, whereas it became temperature-dependent with increasing pH. This unusual temperature dependence of K_d' can be explained in terms of the negative, non-zero ΔC_p of the third strand, which may be caused by the temperature-dependent conformational enthalpy change in the third strand at low pH.

The filter binding method was proven to be a powerful tool for studying the thermodynamic and kinetic aspects of triplex formation. It also appears that the method can elucidate the stringency and specificity of triplex formations among mismatched base sequences under a wide range of environmental conditions.

REFERENCES

Arnott, S., & Selsing, E. (1974) *J. Mol. Biol. 88*, 509–521.

Beal, P. A., & Dervan, P. B. (1991) *Science 251*, 14360–1363.

Blake, R. D., & Fresco, J. R. (1966) *J. Mol. Biol. 19*, 145–160.

Blake, R. D., Klolz, L. C., & Fresco, J. R. (1968) *J. Am. Chem. Soc. 90*, 3556–3562.

Borah, B., & Wood, J. L. (1976) *J. Mol. Struct. 30*, 13–20.

Collier, D. A., Mergny, J.-L., Thuong, N. T., & Helene, C. (1991) *Nucleic Acids Res. 19*, 4219–4224.

Cooney, M., Czermuszewicz, G., Postel, E. H., Flint, S. J., & Hogan, M. E. (1988) *Science 241*, 456–459.

Craig, M. E., Crothers, D. M., & Doty, P. (1971) *J. Mol. Biol. 62*, 383–401.

de los Santos, C., Rosen, M., & Patel, D. (1989) *Biochemistry 28*, 7282–7289.

Durand, M., Peloille, S., Thuong, N. T., & Maurizot, J. C. (1992) *Biochemistry 31*, 9197–9204.

Griffin, L. C., & Pervan, P. B. (1989) *Science 345*, 967–971.

Grigoriev, M., Praseuth, D., Robin, P., Herman, A., Saison-Behmoaras, T., Dautry-Varat, A., Thuong, N. T., Helene, C., & Harel-Bellan, A. (1992) *J. Biol. Chem. 267*, 3389–3395.

Hampel, K. J., Grosson, P., & Lee, J. S. (1991) *Biochemistry 30*, 4455–4459.

Holcomb, N. D., & Tinoco, I., Jr. (1965) *Biochemistry 3*, 121–133.

Ito, T., Smith, C. L., & Canter, C. (1992) *Proc. Natl. Acad. Sci. U.S.A. 89*, 495–498.

Kiessling, L. L., Griffin, L. C., & Dervan, P. B. (1992) *Biochemistry 31*, 2829–2834.

Kohwi, Y., & Kohwi-Shigematu, T. (1991) *Genes. Dev. 5*, 2547–2554.

Krawczyk, B. C., Milligan, J. F., Wadwani, S., Moulds, C., Froehler, B. C., & Matteucci, M. D. (1992) *Proc. Natl. Acad. Sci. U.S.A. 89*, 3761–3764.

Lyamihov, V. I., Mirkin, S. M., Frank-Kamenetskii, M. D., & Cantor, C. R. (1988) *Nucleic Acids Res. 16*, 2165–2187.

Macaya, R. F., Schultze, P., & Feigon, J. (1992) *J. Am. Chem. Soc. 114*, 781–783.

McShan, W. M., Rossen, R. D., Laughter, A. H., Trial, J., Kessler, D. J., Zendegri, J. G., Hogan, M. E., & Orson, F. M. (1992) *J. Biol. Chem. 267*, 5712–5721.

Maelwyn-Hughes, E. A. (1961) in *Physical Chemistry*, 2nd ed., pp 1147–1155, Pergamon Press, Oxford.

Maher, L. J. (1992) *Biochemistry 31*, 7587–7594.

Maher, L. J., Dervan, P. B., & Wold, B. J. (1990) *Biochemistry 29*, 8820–8826.

Maher, L. J., Dervan, P. B., & Wold, B. (1992) *Biochemistry 31*, 70–81.

Mergny, J.-L., Sun, J.-S., Rougee, M., Montenay-Garestier, T., Barcelo, F., Chomilier, J., & Helene, C. (1991) *Biochemistry 30*, 9791–9798.

Moser, H. E., & Dervan, P. B. (1987) *Science 238*, 645–650.

Nielsen, P. E., Egholm, M., Berg, R. H., & Buchardt, O. (1991) *Science 254*, 1497–1500.

Perrouault, L., Asseline, U., Rivalle, C., Thuong, N. T., Bisagni, E., Giovannangeli, C., Le Doan, T., & Helene, C. (1990) *Nature 344*, 358–360.

Pilch, D. S., Levenson, C., & Shafer, R. H. (1990) *Proc. Natl. Acad. Sci. U.S.A. 87*, 1942–1946.

Plum, G. E., Park, Y.-W., Singleton, S. F., Dervan, P. B., & Breslauer, K. J. (1990) *Proc. Natl. Acad. Sci. U.S.A. 87*, 9436–9440.

Porschke, D., & Eigen, M. (1971) *J. Mol. Biol. 62*, 491–512.

Postel, E. H., Flint, S. J., Kessler, D. J., & Hogan, M. (1991) *Proc. Natl. Acad. Sci. U.S.A. 88*, 8227–8231.

Privalov, P. L., & Khechinashvili, N. N. (1974) *J. Mol. Biol. 86*, 665–684.

Radhakrishnan, I., Patel, D. J., & Gao, X. (1992) *Biochemistry 31*, 2514–2523.

Rajagopal, P., & Feigon, J. (1989) *Nature 339*, 637–640.

Riggs, A. D., Bourgeois, S., & Cohen, M. (1970) *J. Mol. Biol. 53*, 401–417.

Roberts, R. W., & Crothers, D. M. (1991) *Proc. Natl. Acad. Sci. U.S.A. 88*, 9397–9401.

Robinson, H., van der Marel, G. A., van Boom, J. H., & Wang, A. H.-J. (1992) *Biochemistry 31*, 10510–10517.

Ross, P. D., & Sturtevant, J. M. (1962) *J. Am. Chem. Soc. 84*, 4503–4507.

Rougee, M., Faucon, B., Mergny, J. L., Barcelo, F., Giovannangeli, C., Garestier, T., & Helene, C. (1992) *Biochemistry 31*, 9269–9278.

Saenger, W. (1984) in *Principles of Nucleic Acid Structure*, Chapter 13, Spring-Verlag, New York.

Singleton, S. F., & Dervan, P. B. (1992a) *J. Am. Chem. Soc. 114*, 6957–6965.

Singleton, S. F., & Dervan, P. B. (1992b) *Biochemistry 31*, 10995–11003.

Strobel, S. A., Doucette-Stamm, L. A., Riba, L., Housman, D. E., & Dervan, P. B. (1991) *Science 254*, 1639–1642.

Wells, R. D., Collier, D. A., Hanvey, J. C., Shimizu, M., & Wohlrab, F. (1988) *FASEB J. 2*, 2939–2949.

Xodo, L. E., Manzini, G., & Quadrifoglio, F. (1990) *Nucleic Acids Res. 18*, 3557–3564.

Xodo, L. E., Manzini, G., Quadrifoglio, F., van der Marel, G. A., & van Boom, J. H. (1991) *Nucleic Acids Res. 19*, 5625–5631.

Yoon, K., Hobbs, C. A., Koch, J., Sardaro, M., Kutny, R., & Weis, A. L. (1992) *Proc. Natl. Acad. Sci. U.S.A. 89*, 3840–3844.